N-64-5

SOLID ROCKET PLANT

ANALYSIS OF PROPELLANT IGNITION, AND ITS APPLICATION TO MOTOR INITIATION

By

R. L. Lovine, L. Y. Fong, B. E. Paul

Technical Memorandum 235 SRP

4 November 1963

428270

AEROJET
GENERAL TIRE
GENERAL

AEROJET-GENERAL CORPORATION

SACRAMENTO, CALIFORNIA

8700

ANALYSIS OF PROPELLANT IGNITION, AND ITS APPLICATION TO MOTOR INITIATION

By

R. L. Lovine, L. Y. Fong, B. E. Paul

Technical Memorandum 235 SRP

4 November 1963

TABLE OF CONTENTS

ANALYSIS OF PROPELLANT IGNITION, AND ITS APPLICATION TO MOTOR INITIATION

R. L. Lovine, L. Y. Fong, B. E. Paul

Aerojet-General Corporation

ABSTRACT

In order to relate igniter energy output to motor ignition a model of solid propellant ignition is given. Difficulties inherent in the non-linear partial differential equations of heat and mass diffusion describing the ignition system prevent the model from being completely analytical. However, certain results are derived from the equations, and when combined with arc-image furnace ignitability data, a reasonably coherent view of the process is obtained. Numerous examples of ignitability data are given.

Analysis of heat and mass transfer from igniter to motor grain is given for the case of propellant type igniter. This analysis, along with the pertinent ignitability data, is applied to ignition of the 2nd stage Minuteman motor.

I. INTRODUCTION

In order to predict performance and specify reliability of solid propellant rocket ignition systems, it has been found necessary to have a model of propellant ignition. In other words, rational design of an ignition system implies that igniter output be based on ignition energy and pressure requirements for a particular propellant, perhaps having specified surface preparation, or having undergone prescribed environmental conditioning.

Attempts to establish ignition energy requirements have led to various models of the ignition process. Until recently, a thermal model of ignition, including heat generation, yielded the usual method of analysis. This model, which is adequately described in References (1) through (5), is essentially based on the assumption of solid phase reactions usually taken as first order. Gas phase reactions are neglected. Using this model, investigators were able to explain data acquired from ignition tests where hot wire, hot plate, and hot bath apparatus were used as heat sources. These types of apparatus virtually exclude the ambient atmosphere, and so diffusion, as an ignition parameter.

In the ignition analysis given here, the thermal model of ignition is taken as the starting point. Results found by investigators applying this model will be used liberally. An extension of the thermal model will be made in order to account for known pressure sensitivity when ignition occurs in a gaseous medium. The problem of heat and mass diffusion in a reacting gas is found to be extremely complex, but an approximation can be made which will yield some information.

Test data obtained by means of the Stanford Research Institute arc-image furnace are given. This ignitability data has been obtained for a variety of propellant compositions, having several surface conditions.

Finally, igniter energy and pressure output is defined by means of mass and energy balances applied to a propellant ignition system. The entire analysis is applied to the ignition of the Minuteman 2nd stage motor. An ignition safety factor is defined and computed for the stage in the ignition train consisting of motor ignition from main igniter charge.

II. PROPELLANT IGNITION

Recent ignition research has demonstrated that the ignition process is pressure dependent (Reference (6), (7) and (8)). Hence any ignition model must consider both propellant surface phenomena and vapor phase reactions in the vicinity of the propellant surface. In the model presented here it will be assumed first that the solid propellant undergoes a primary decomposition from solid into gases, which undergo further reactions before the final combustion products are reached. The primary decomposition is a result of a heat flux at the propellant surface which is sufficiently high so that only a very thin layer of propellant is affected before ignition occurs. In this case heat generation by solid phase reaction need not be considered. Secondly, gas phase reactions of decomposition products are assumed to occur which will, under good ignition conditions, transfer a sufficient amount of energy back to the propellant surface to sustain the combustion of the solid propellant.

The time interval between igniter flux onset, when the propellant surface is first exposed to the igniter heat flux, and the instant when

surface decomposition begins, is called the thermal induction interval. It is characterized by accumulation of heat in the propellant, establishment of a temperature gradient at the exposed surface, and finally surface decomposition.

The time interval between commencement of propellant surface decomposition, under the action of the igniter induced heat flux, and self-sustaining combustion, is called the chemical induction interval. It is characterized by an accumulation of active, gas phase species in the vicinity of the propellant surface, further exothermic reactions of the species, and finally, under good ignition conditions, a reaction rate sufficiently high to cause self-sustained combustion of the solid propellant. It must be emphasized here that time-to-ignition will be the sum of thermal and chemical induction intervals.

The two pertinent ignition time intervals, thermal and chemical induction, will be treated separately. It will be found that the value of the thermal induction interval can be calculated with resonable certainty. In contrast, the only information gained on the chemical induction interval will be its dependence on such parameters as ambient pressure. The reasons for this are the complexity, and non-linearity, of the partial differential equations governing mass and energy transfer in a gas undergoing exothermic chemical reactions. Analytic solution of the equations appears impossible, and numerical solution usually obscures significant trends. Fortunately, data made available through arc-image furnace ignition tests determine time to ignition at a variety of ambient pressures. The thermal induction interval may be calculated and subtracted from the test data, with the

difference being the chemical induction interval. Combining this experimental data with the analysis in this section permits extension of the data so that the chemical induction interval can be obtained for other significant ignition parameters. That is to say, combining the meager analytical results with experimental data from ignition tests will result in a fairly comprehensive picture of gas phase ignition.

A. THERMAL INDUCTION INTERVAL

When solid rocket propellant is exposed to a high intensity heat flux, as in the case of normal ignition, the surface of the propellant is assumed to undergo a primary decomposition from solid into gases. These primary decomposition products are assumed to react further before final decomposition products are reached. In normal ignition, the igniter induced heat flux is sufficiently high so that only a very thin layer of propellant is affected before ignition occurs (References (1) and (2)) and in this case heat generation by solid phase reactions need not be considered. The time required to bring about primary surface decomposition, which is identical to the thermal induction interval, is calculated by a simple thermal analysis at the propellant surface. Use of a single, constart ignition temperature is based on results found by Altman and Grant (Reference (3)).

As an illustration consider the case of an igniter with a nearly constant mass flow rate, and hence a nearly constant heat flux. When the gas temperature of the igniter combustion products is high the heat flux at the propellant surface is nearly independent of surface temperature. In this case the transient temperatures inside the propellant grain are given by,

$$T(x,t) - T_a = Y\left\{(2/\sqrt{\pi}) \exp(-X^2) - 2X \operatorname{erfc} X\right\} \quad (1)$$

The dimensionless numbers are,

$$Y = \dot{q}\sqrt{\alpha t}/k$$

$$X = x/2\sqrt{\alpha t}$$

where

$T(x,t)$ = temperature at position x, and time t

T_a = initial ambient temperature

$\dot{q}$ = igniter induced heat flux

α = propellant diffusivity

k = propellant conductivity

Now let t_o be the time required to raise the critical layer thickness, x_o, to the ignition temperature, T_i. Then from Eq. (1)

$$T_i - T_a = Y_o\left\{(2/\sqrt{\pi}) \exp(-X_o^2) - 2X_o \operatorname{erfc} X_o\right\} \quad (2)$$

$$Y_o = \dot{q}\sqrt{\alpha t_o}/k$$

$$X_o = x_o/2\sqrt{\alpha t_o}$$

Equation (2) then, establishes relations between the thermal induction interval, t_o, the ambient temperature, T_a, and the various propellant and igniter properties.

B. CHEMICAL INDUCTION INTERVAL

The chemical reaction rate will be taken as first order which is in agreement with a burning rate exponent of one-half. The equations of mass and energy conservation, for an immobile system, become respectively,

$$\frac{\partial \tilde{C}}{\partial t} = D \frac{\partial^2 \tilde{C}}{\partial x^2} - Z_1 \tilde{C} e^{-E/RT} \tag{3}$$

$$\frac{\partial T}{\partial t} = \bar{\alpha} \frac{\partial^2 T}{\partial x^2} + \frac{T_m Z_1 \tilde{C} e^{-E/RT}}{\rho} \tag{4}$$

where

$\tilde{C}$ = concentration of reactants

Z_1 = pre-exponential factor

E = activation energy

R = universal gas constant

T_m = explosion temperature

D = mass diffusivity

$\bar{\alpha}$ = gas thermal diffusivity

ρ = mixed gas density

x = distance from propellant surface

The concentration of reactants, $\tilde{C}$, is defined in terms of its partial pressure, P_1, by

$$\tilde{C} = (P_1/bT)$$

where b is the specific gas constant.

In order to obtain a rough approximation to the reactant weight density buildup before ignition the mass balance, Eq. (3), will be solved assuming constant temperature. In this case, Eq. (3) and the boundary conditions are,

$$\frac{\partial \tilde{C}}{\partial t} = D \frac{\partial^2 \tilde{C}}{\partial x^2} - K_1 \tilde{C} \tag{5}$$

$$K_1 = Z_1 e^{-E/RT}$$

$$-D \frac{\partial \tilde{C}}{\partial t} = \varphi \text{ , constant mass flux}$$

$$\tilde{C} = 0, \; x \geq 0, \; t = 0$$

The mass flux, φ, is approximately related to the heat flux, $\dot{q}$, by,

$$\varphi = \frac{\dot{q}}{c(T_i - T_a)} = r\rho_o$$

where c is the heat capacity of the solid propellant, r is the linear regression rate of the propellant surface, and ρ_o the propellant density. Existence of such a mass flux prior to ignition has been verified by arc-image furnace ignition tests (Reference (6)).

The solution to Eq. (5) at the surface, x = 0, is,

$$C = \frac{\varphi}{\sqrt{K_1 D}} \operatorname{erf} \sqrt{K_1 t} \tag{6}$$

Before ignition occurs, the temperature rise near the surface should be small. Then the reaction rate varies directly with concentration,

$\tilde{C}$. This leads to the assumption of a critical reactant weight density, C*, for self-sustaining combustion, and t_c, a critical time, or chemical induction period. Then, from Eq. (6),

$$\operatorname{erf}\sqrt{K_1 t_c} = \frac{\sqrt{K_1 D}}{r\rho_o} C^*$$

The mass diffusivity, D, is taken proportional to the ratio of viscosity and gas density when inert and active species are molecularly similar, and approximately,

$$D = \mu/\rho$$

Using this relation, the pressure dependence of the chemical induction interval can be established, and is

$$\operatorname{erf}\sqrt{K_1 t_c} = \frac{\sqrt{K_1 RT}}{\varphi\sqrt{p}} C^* = \frac{W}{\sqrt{p}} \qquad (7)$$

where W is defined by Eq. (7).

The plot of $\left(K_1 t_c\right)$ against the inverse square of the right hand side of Eq. (7), which is shown in Figure (1), shows that for a sufficiently low pressure the chemical induction interval approaches infinity. In other words, for a given propellant there is a pressure below which ignition will not occur. Furthermore, for moderate pressures the chemical induction interval approaches zero. Inspection of test data shows that for ambient pressure exceeding about six atmospheres, the chemical induction interval is nearly non-existent for polyurethane composite propellant. By conducting ignitability tests at high pressure, values of the thermal induction interval are isolated, and by using steady state values of the ignition temperature, the value of the critical layer thickness is obtained.

IGNITION PRESSURE - CHEMICAL INDUCTION INTERVAL

THEORETICAL DEPENDENCE

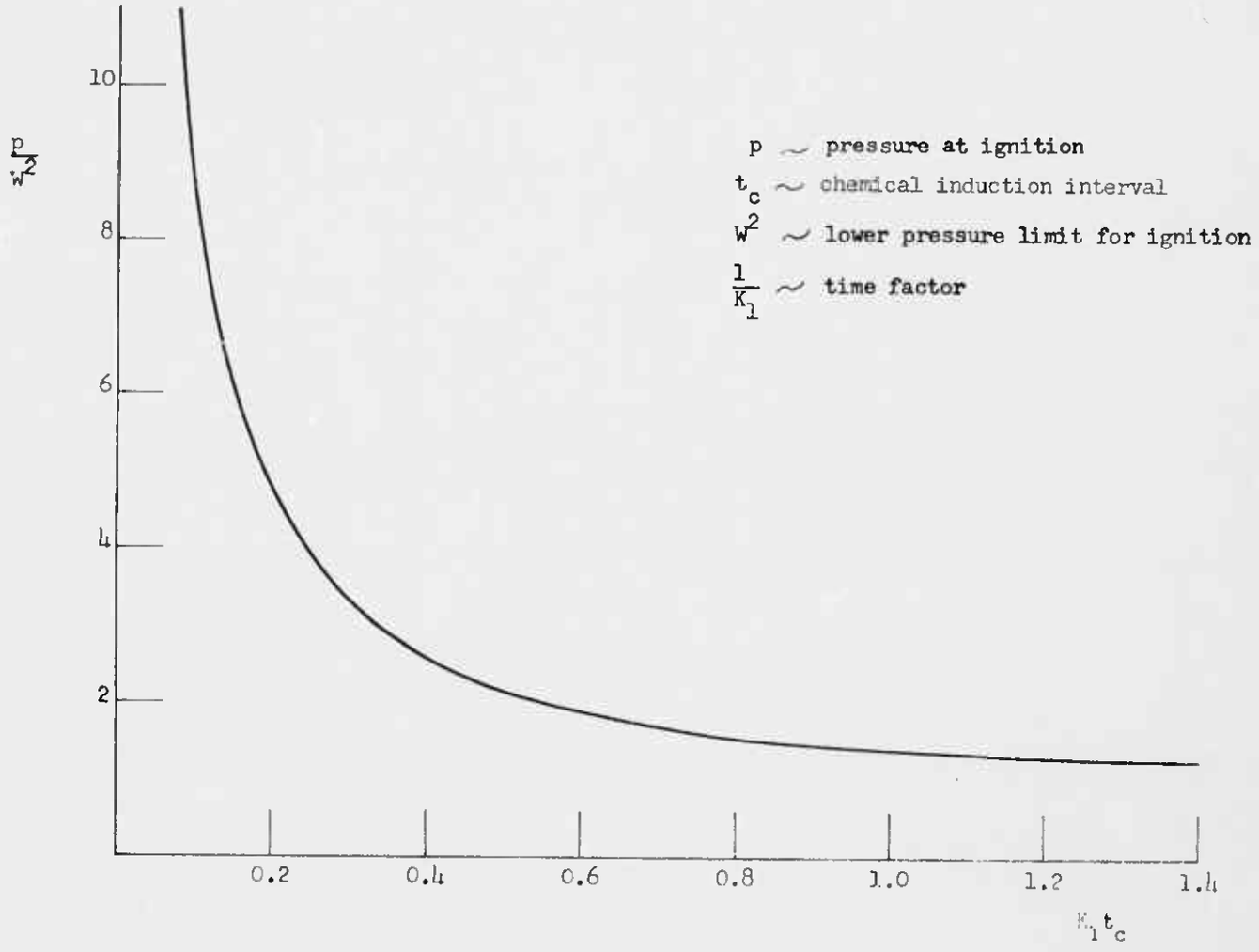

Figure 1

Ignitability tests conducted near the lower ignition pressure threshold level will allow determination of the pressure parameter, W^2, (Eq. (7)). An additional ignitability determination in the pressure range between zero and infinite chemical induction interval, will suffice to fix the entire ignitability curve with some degree of certainty.

C. IGNITABILITY DATA

Ignitability measurements have been made on a number of propellant compositions, under several conditions of heat flux and environmental pressure. The device used to acquire the data was an arc-image furnace, operated by the Stanford Research Institute. Propellant samples, in a fixed pressure environment of gaseous nitrogen, are tested by exposing them to a beam of radiant energy of known intensity for a fixed duration. Time to ignition is reported as the average over four successful ignitions and four failures.

Inspection of the arc-image furnace test data shows that the ignition pressure threshold level is in the vicinity of one atmosphere for many propellants, as is seen in Figures (2) and (3). But in the case of ANB-3066 LC, the level is much lower, in the vicinity of 4 psia, (Figures (6) and (7)). The critical surface layer thickness seems to be proportional to the average oxidizer particle size. Normally, several oxidizer grinds are used in any given propellant composition, making comparison difficult. However, the critical layer thickness is about 30 microns for ANP-2655 AF, with its relatively fine oxidizer blend, and about 100 microns for ANB-3066 LC, which has a relatively coarse oxidizer blend.

The ignitability data is graphed in Figures (2) through (7). Short descriptions of the graphs follow.

Figures (2) and (3): Environmental pressure reported for ignition is plotted against the time to ignition for a variety of propellants. Data plotted in Figure (2) was obtained at a heat flux of 70 cal/cm^2/sec, while data plotted in Figure (3) was obtained at 20 cal/cm^2/sec. The propellant surface preparation for these tests was that of a freshly cut surface, which has become a standard for this type of test.

Figures (4) and (5): Data acquired on surface effects are shown on these two graphs. For each of two types of propellant compositions, a variety of test specimens were prepared, using different methods of surface preparation. The specimens were tested at pressure levels of one, two and three atmospheres. Generalities are difficult to arrive at from the data obtained. However, surfaces prepared by casting against Styrofoam, and then stripping the Styrofoam from the surface after cure, appear most readily ignitable. This may be either a result of a more favorable surface composition, or a consequency of an increase in radiation absorption caused by extreme surface roughness.

Specimens having surfaces cast against RTV-60, a silicone rubber mold release composition, were also readily ignitable compared with the standard cut surface preparation. The RTV-60 surface is smooth compared with that obtained from stripped Styrofoam. Figure (5) shows a remarkable fact concerning ANB-3066 LC propellant composition, namely the near pressure insensitivity of its ignitability over a pressure range of one to three atmospheres.

Figures (6) and (7): The ignitability of one propellant, ANB-3066 LC having a surface cast against RTV-60, was found over a wide

TIME TO IGNITION AT FLUX OF 70 CAL/CM^2 SEC
VARIOUS PROPELLANTS CUT SURFACE

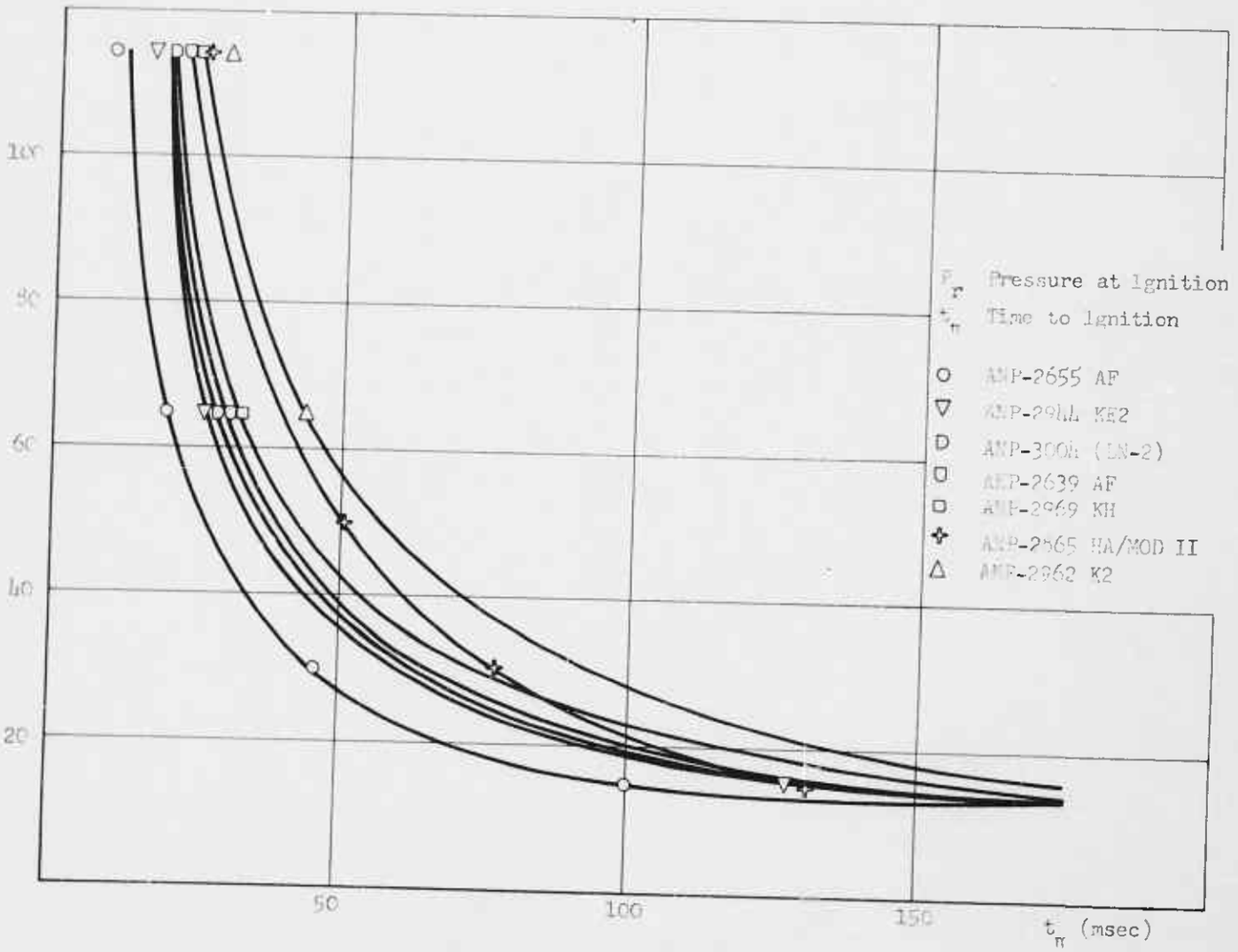

Figure (2)

TIME TO IGNITION AT FLUX OF 20 CAL/CM^2 SEC
VARIOUS PROPELLANTS CUT SURFACE

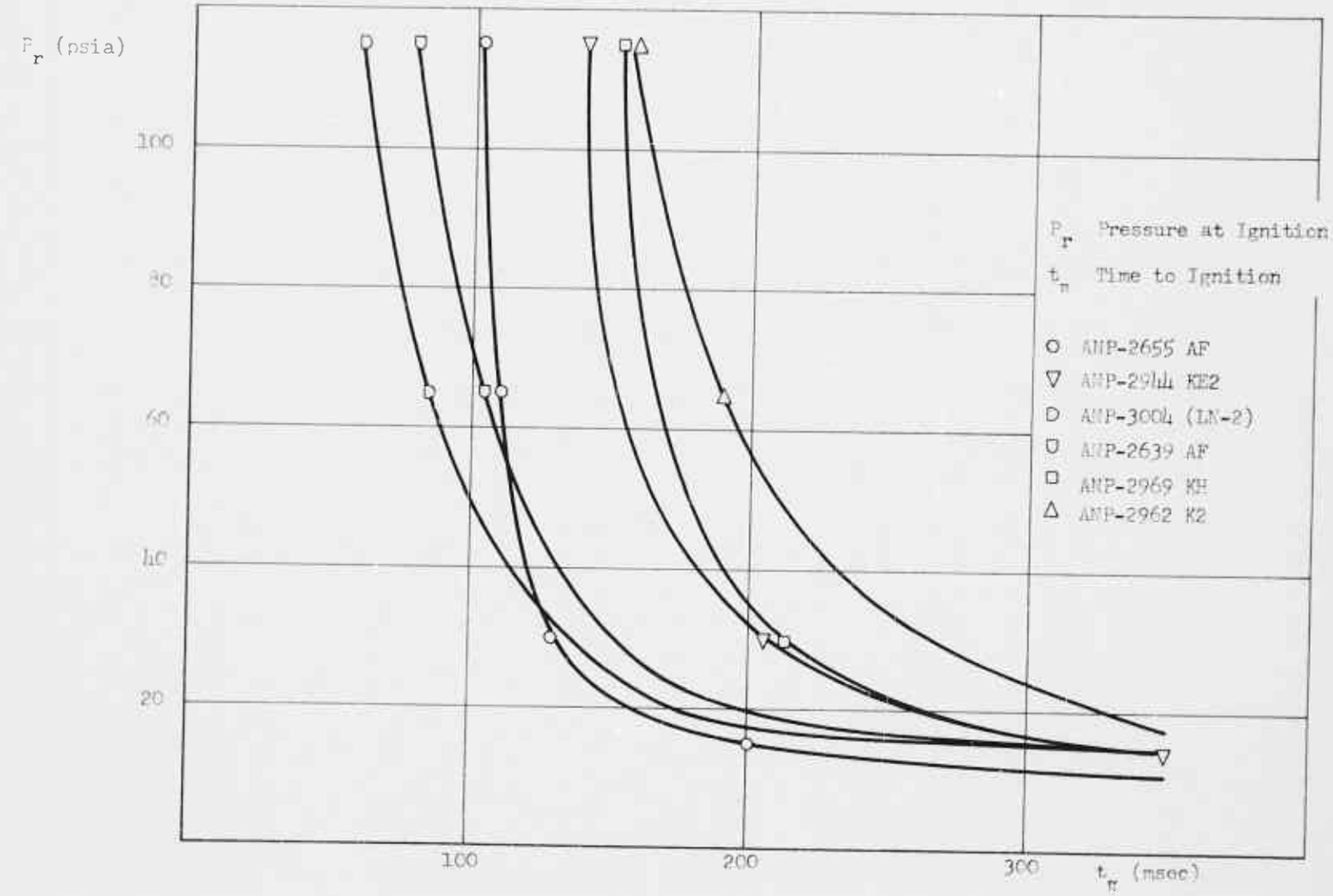

Figure (2)

TIME TO IGNITION AT FLUX OF 70 CAL/CM^2 SEC - ANP-2864 PB/MOD II
VARIOUS SURFACE PREPARATIONS - 1, 2, and 3 ATMS.

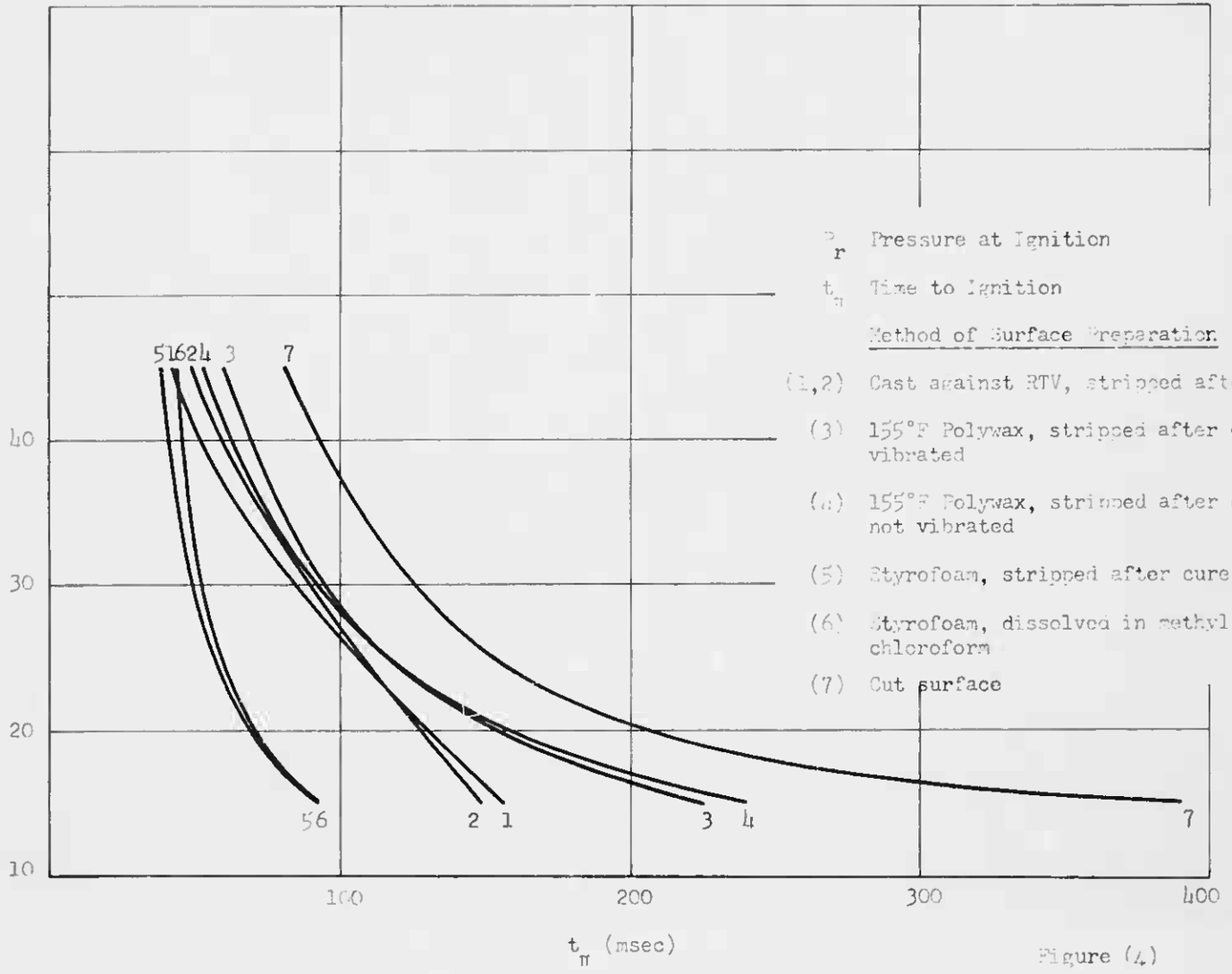

Figure (4)

TIME TO IGNITION AT FLUX OF 70 CAL/CM^2 SEC - ANB-3066 LC
VARIOUS SURFACE PREPARATIONS - 1, 2, and 3 ATMS.

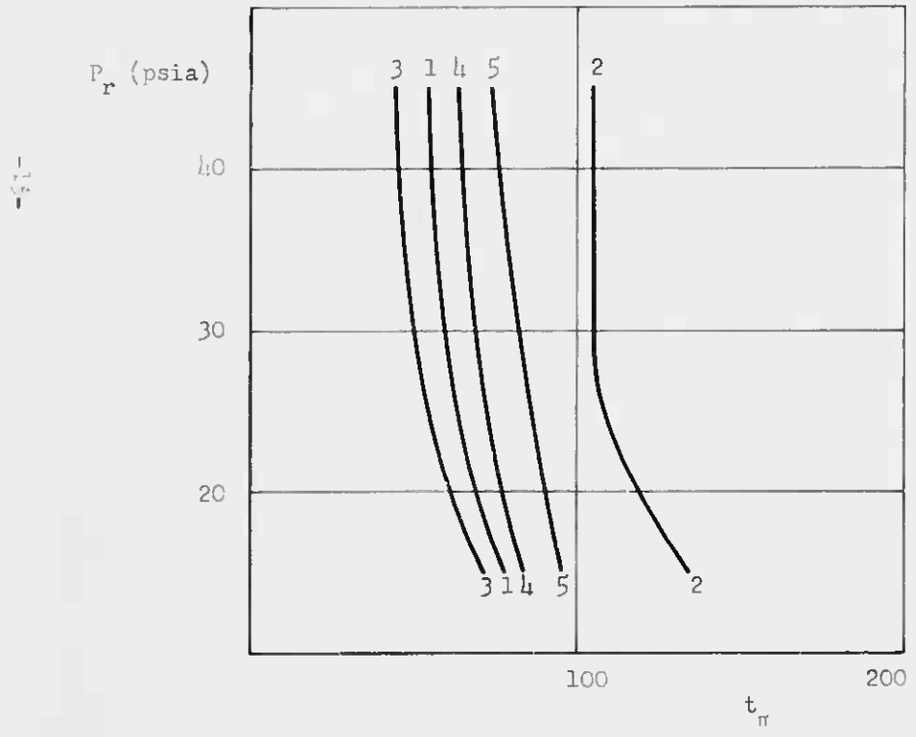

P_r Pressure at Ignition

t_π Time to Ignition

Method of Surface Preparation

(1) Cast against RTV, stripped after cure

(2) 155°F Polywax stripped after cure, vibrated

(3) Styrofoam, stripped after cure

(4) Styrofoam, dissolved with methyl chloroform

(5) Cut Surface

Figure (5)

TIME TO IGNITION AT FLUX OF 70 CAL/CM^2 SEC - ANB-3066 LC

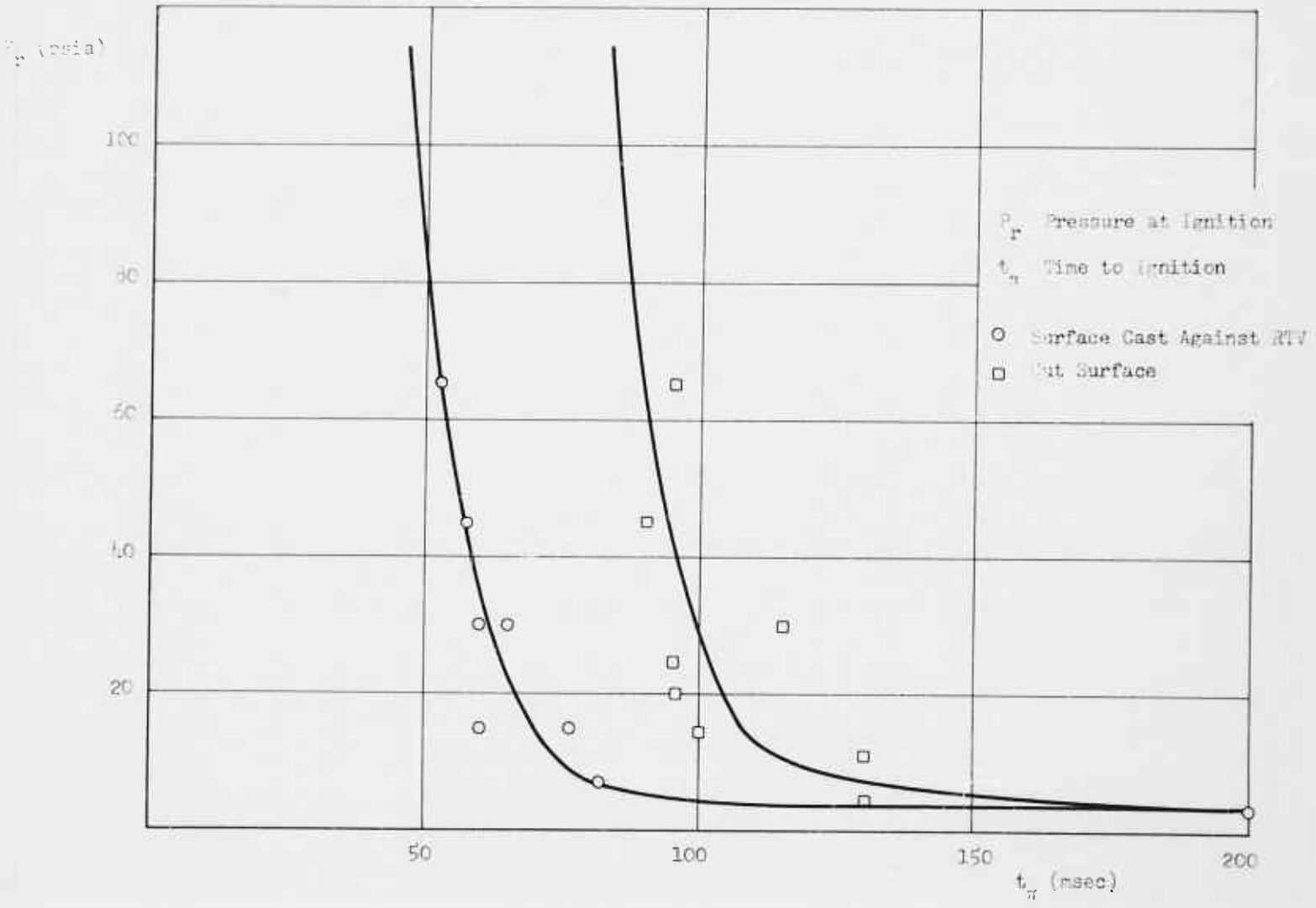

Figure (6)

TIME TO IGNITION AT FLUX OF 40 CAL/CM^2 SEC - ANB-3066 LC

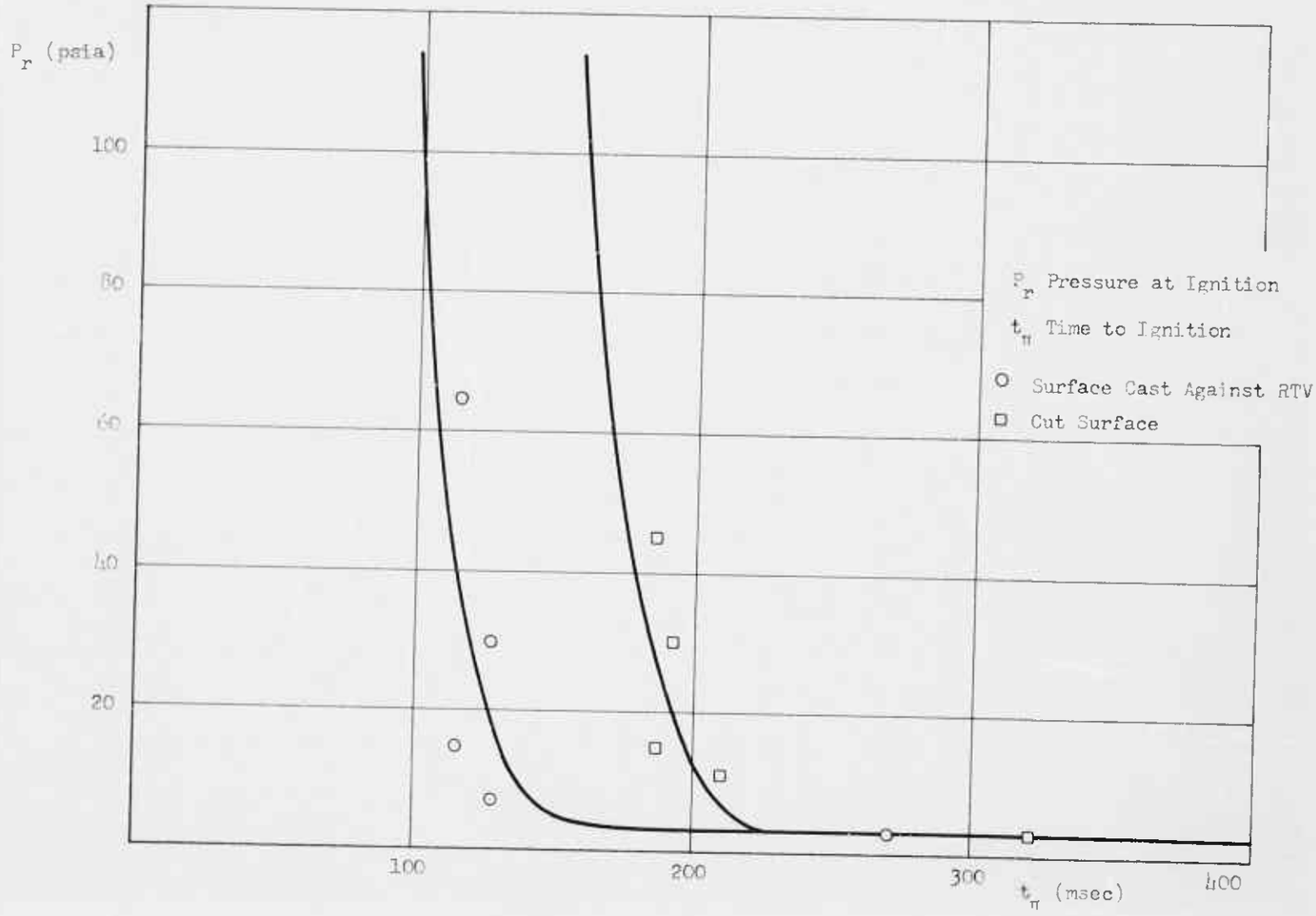

Figure (7)

range of pressure, 1.5 psia up to 65 psia, and at flux levels of 70 and 40 cal/cm^2/sec. Specimens of the same propellant having a fresh cut surface were also tested for comparative purposes.

As noted previously, this test sequence showed that propellant having a surface cast against RTV-60 is more readily ignitable than one having a surface prepared by cutting. These data also show an ignition pressure threshold of about 4 psia for this propellant composition, which compares well with the commonly found level of about one atmosphere.

Figures (8), (9), and (10): Illustrations of the physical variations brought about by various methods of surface preparation are shown in forty power photomicrographs of some of the samples tested. Most specimens, for example those cast against RTV-60, the cut surface, and those cast against 155°F Polywax, have a smooth appearing surface. However, the surface cast against 155°F Polywax has a distinct coating of the wax remaining on the surface. Even though all of these propellant samples have similar appearances, the results of the ignitability test show a real difference. Samples of the remaining type of surface preparation, namely that resulting from casting against styrofoam, were jagged and obviously easy to ignite regardless of method of foam removal.

III. IGNITER INDUCED MOTOR PRESSURIZATION AND GRAIN IGNITION

The combustion products from the igniter pressurize the port volume of the motor and transfer heat to the grain surface. In this section expressions will be found from which the igniter induced chamber pressure may be obtained. And for a particular case, that of a

MAGNIFICATION
100 X

AMP-2266, HG/Mod II
Cast against RTV,
stripped after cure

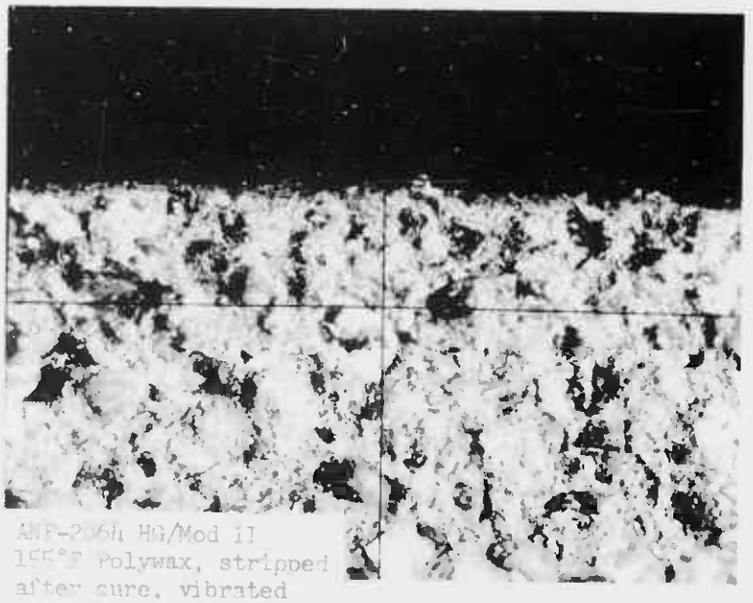

AMP-2266 HG/Mod II
155°F Polywax, stripped
after cure, vibrated

Figure 8

MAGNIFICATION
40 X

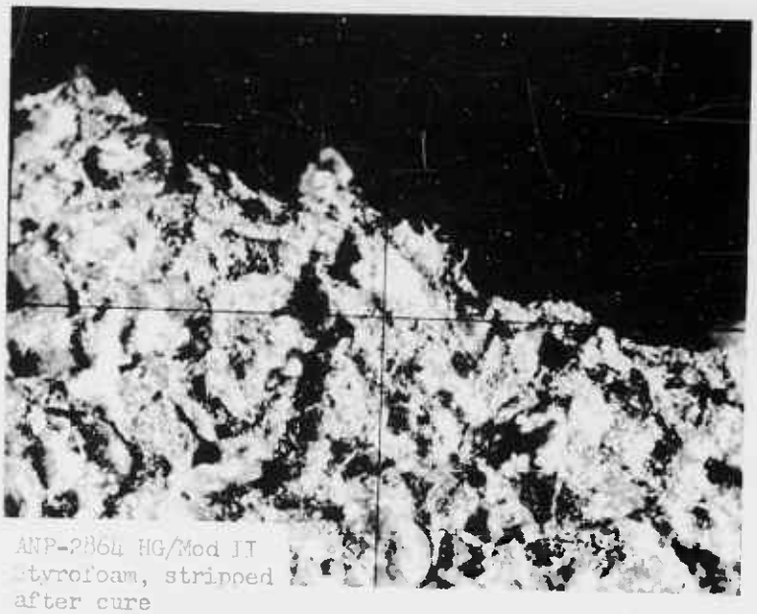

ANP-2864 HG/Mod II
Styrofoam, stripped
after cure

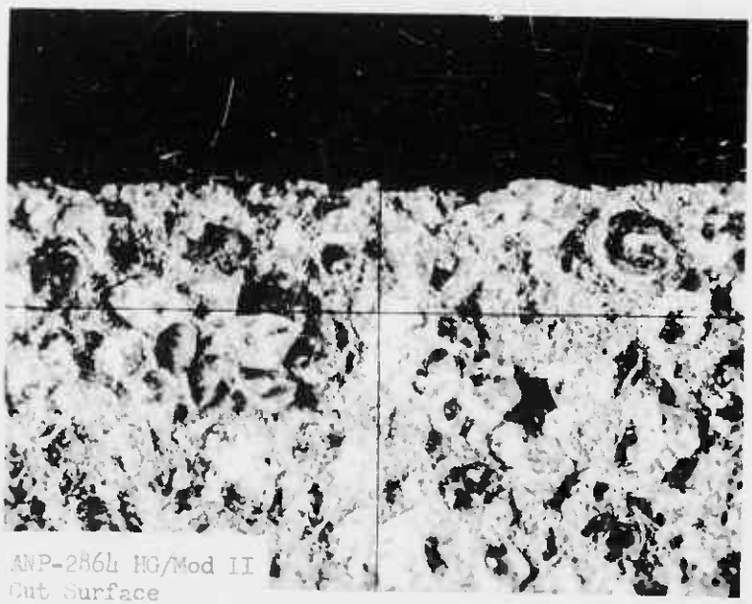

ANP-2864 HG/Mod II
Cut Surface

Figure 9

MAGNIFICATION
40 X

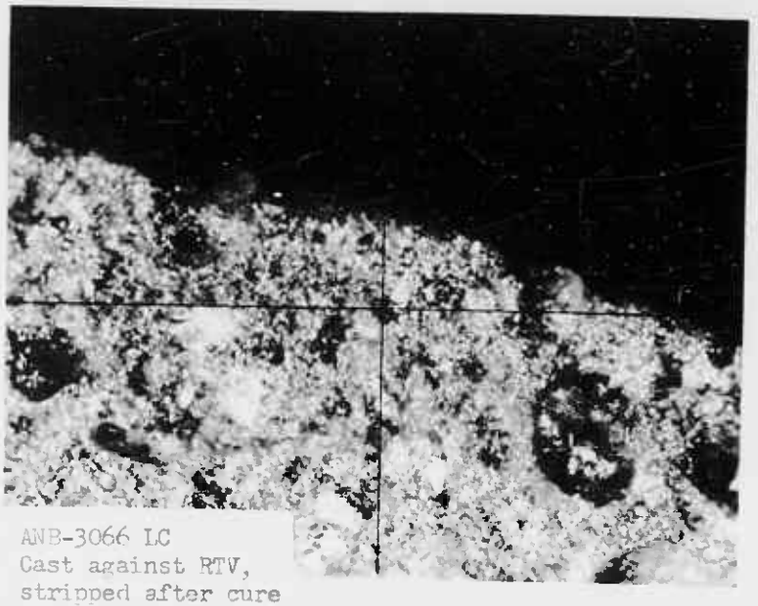

ANB-3066 LC
Cast against RTV,
stripped after cure

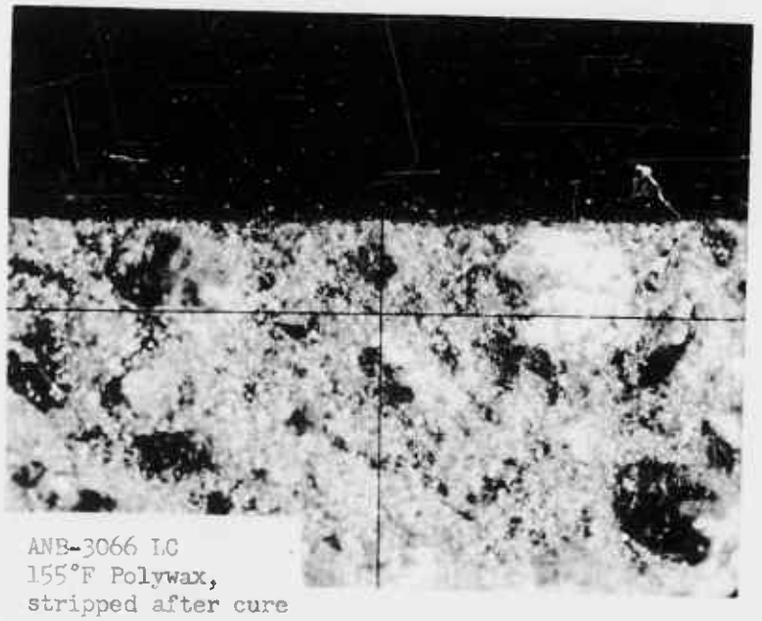

ANB-3066 LC
155°F Polywax,
stripped after cure

Figure 10

controlled flow igniter with a propellant pyrotechnic, the expression for heat flux to the propellant grain is found. These two items, pressurization and heat flux, are combined with ignitability data to provide an analysis of 2nd stage Minuteman ignition.

A. CONSERVATION EQUATIONS

Both mass and energy are transferred as the combustion products of the igniter flow into the port volume of the motor. In this section the descriptive equations of mass and energy conservation will be given. It will be found that the full set of descriptive equations are too cumbersome to solve analytically. Certain simplifying assumptions will be introduced, and the simplified equations solved.

Mass Balance: The thermodynamic system is the motor port volume (combustion chamber), and the time interval is taken from initiation of the igniter up to the instant of grain ignition. Combustion of the igniter pyrotechnic causes a mass flow into the system. Simultaneous with pressurization of the port volume, there is a mass flow out the motor nozzle. The mass balance will be then, an equation involving three terms, the statement being as follows. The rate of change of mass in the system equals the mass flow rate from the igniter minus the mass flow rate out the nozzle. Symbolically,

$$\dot{m}_c = \dot{m}_i - \dot{m}_o \tag{8}$$

where m_c = mass in the system

m_i = mass from the igniter, assumed known

m_o = mass out the nozzle

The "dot" refers to time differentiation.

Flow out the nozzle will be assumed to run full at all times. In other words, the mass flow out the nozzle will be given the same form as in the sonic case. It can be shown (Reference (9)) that when the exit pressure is as high as 75% of the chamber pressure, the mass flow rate is already 90% of maximum under sonic conditions. Then using the sonic flow rate form,

$$\dot{m}_o = \frac{K A_t P_c}{\sqrt{T_c/T_o}}$$

where K = discharge coefficient, and

$$K = \left(\frac{\gamma g}{F}\right)^{1/2} \left(\frac{2}{\gamma + 1}\right)^{\frac{\gamma + 1}{2(\gamma - 1)}}$$

F = igniter combustion product force constant

γ = isentropic constant

A_t = motor throat area

P_c = motor chamber pressure

T_c, T_o = gas temperature in motor chamber and isochoric flame temperature, respectively

The isochoric flame temperature, T_o, is of course, a constant. Chamber temperature, T_c, is expected to be a variable.

The mass in the system is obtained from the equation of state of a perfect gas, effects of co-volume and incondensibles being accounted for in the igniter combustion product force constant, F, (Reference (10)).

Then

$$\dot{m}_c = \frac{V}{F} \frac{d(P_c/\theta)}{dt}$$

where V = motor chamber volume

$\theta = T_c/T_o$

Using the above expressions of mass terms, the equation of conservation of mass now reads,

$$\frac{V}{F} \frac{d(P_c/\theta)}{dt} = \dot{m}_i - \frac{K A_t P_c}{\sqrt{\theta}} \tag{9}$$

Energy Balance: In the system already described, the statement of the energy balance is as follows. The rate of change of energy in the system equals the energy flow rate from the igniter, minus the sum of energy flow out the motor nozzle and heat losses to the walls of the combustion chamber. The heat lost to the walls of the combustion chamber includes heat transferred to the propellant grain as well as to inert parts. Symbolically,

$$\dot{E}_c = \dot{E}_i - \dot{E}_o - \dot{H} \tag{10}$$

where E_c = energy in the motor chamber

E_i = energy from igniter

E_o = energy out nozzle

H = heat lost to walls of enclosure

The "dot" refers to time differentiation.

With the exception of the heat loss rate, $\dot{H}$, the energy terms correspond to the mass terms, and in these terms, Eq. (10) is,

$$C_v \frac{d}{dt} (T_c m_c) = C_p T_i \dot{m}_i - C_p T_c \dot{m}_o - \dot{H} \qquad (11)$$

where the additional terminology means

C_v, C_p = isochoric and isobaric heat capacities of igniter combustion product, respectively

T_i = flame temperature in the igniter combustion chamber

If the temperature in the igniter chamber has achieved equilibrium, then $T_o = \gamma T_i$. The energy balance, Eq. (11), rewritten in terms of familiar parameters is,

$$\frac{V}{F} \frac{dP_c}{dt} = \dot{m}_i - \gamma\sqrt{\theta^{-1}} K A_t P_c - \frac{\dot{H}}{Q} \qquad (12)$$

where $Q = C_v T_o$

Heat Loss Rate: The heat loss rate, $\dot{H}$, will be estimated on the basis of a convective heat flux from the igniter combustion product to walls enclosing the combustion chamber. In the case of a propellant igniter the convective type flux is most significant. The Nusselt relation, in terms of igniter mass flow rate and a Prandlt number near unity, is, from Reference (11),

$$\frac{hd}{k} = 0.023 \left(\frac{\dot{m}_i d}{\mu g A_f} \right)^{.8}$$

where h = heat transmission coefficient

d = hydraulic diameter in motor chamber

μ = dynamic viscosity

k = gas conductivity

$\dot{m}_i$ = mass flow rate in the chamber, taken equal to igniter mass flow rate

A_f = flow area in chamber

The heat loss rate, $\dot{H}$, heat flux, $\dot{q}$, and heat transmission coefficient are related through,

$$\dot{H} = A_s \dot{q} = A_s h \, (T_c - T_s) \tag{13}$$

where A_s is the total exposed surface area of the walls enclosing the combustion chamber, and T_s is an average wall temperature during the process. Average values will be used for most thermodynamic parameters, which is adequate since the heat loss correction is a second order effect.

Several relationships will be used to write the heat transmission coefficient in terms of parameters used previously. From kinetic gas theory the gas conductivity is related to dynamic viscosity and heat capacity by,

$$k = \frac{9\gamma - 5}{4} \, C_v \mu g$$

Then from Eq. (13)

$$\frac{\dot{H}}{Q} = \left[.023 \left(\frac{9\gamma - 5}{4} \right) \left(\frac{\mu g A_f}{d} \right)^{.2} \left(\frac{A_s}{A_f} \right) \right] \dot{m}_i^{.8} \, (\theta - \theta_s) \tag{14}$$

or

$$\frac{\dot{H}}{Q} = \Gamma \, \dot{m}_i^{.8} \, (\theta - \theta_s) \tag{15}$$

where θ_s is the ratio of average surface temperature, T_s, to the isochoric flame temperature, T_o, and,

$$\Gamma = \left[.023 \left(\frac{9\gamma-5}{4}\right)\left(\frac{\mu g A_f}{d}\right)^{.2} \left(\frac{A_s}{A_f}\right)\right] \tag{16}$$

Substituting this expression into the energy balance, Eq. (12), results in,

$$\frac{V}{F}\frac{dP_c}{dt} = \dot{m}_i - \Gamma \dot{m}_i^{.8}(\theta - \theta_s) - \gamma\sqrt{\theta}\, KA_t\, P_c \tag{17}$$

The mass balance, Eq. (9), is repeated.

$$\frac{V}{F}\frac{d(P_c/\theta)}{dt} = \dot{m}_i - \frac{KA_t\, P_c}{\sqrt{\theta}} \tag{18}$$

A glance at the two conservation equations makes it clear that there are two dependent variables, igniter induced chamber pressure, P_c, and the gas temperature ratio, θ, to be solved for in terms of an independent variable, time. Further, each of the equations contains non-linear terms in a dependent variable, which in effect means the system cannot be solved by elementary methods of integration.

Simplifications: Since the non-linearity of the conservation equations inhibits obtaining a solution by elementary methods, a means of linearizing the equations will be given here. The method consists of approximating the chamber temperature, T_c, and substituting the approximate value into the energy balance, Eq. (17). This will give an approximate energy balance, linear in the dependent variable of chamber pressure.

Consider a total energy balance on the igniter combustion product,

$$C_p T_i m_i = C_p T_c m_i + H \tag{19}$$

where H is the total heat lost to the walls of the enclosure, and m_i is the total igniter charge weight. From Eq. (15),

$$H \sim Q \Gamma m_i^{.8} (\theta - \theta_s)$$

Substituting this expression for total heat lost back into Eq. (19), yields an approximate average value of the temperature ratio,

$$\theta_a = \frac{1 + \frac{\Gamma}{m_i^{.2}} \theta_s}{\gamma + \frac{\Gamma}{m_i^{.2}}} \tag{20}$$

where $\theta_a = T_c/T_o$, constant

The energy equations, Eq. (17), reads then,

$$\frac{V}{F} \frac{dP_c}{dt} = \dot{m}_e - \gamma \sqrt{\theta_a} K A_t P_c \tag{21}$$

which has an integral,

$$P_c = e^{-at} \left\{ P_i + \int_o^t e^a \; b(\tau) \, d\tau \right\} \tag{22}$$

where $\dot{m}_e = \dot{m}_i - \lceil m_i \cdot^{\varepsilon} \theta_a$

$$e = \frac{F}{V} \gamma \sqrt{\theta_a \rceil} K A_t$$

$$b(\tau) = \frac{F}{V} \dot{m}_e(\tau)$$

P_i = initial chamber pressures

IV. APPLICATIONS

In the previous sections, collected arc-image furnace ignition test data has been exhibited. Further, methods for calculeting the igniter induced chamber pressure and heat flux have been found. However, there are certain difficulties in obtaining relations between the arc-image furnace test data, the expression for igniter induced chamber pressure, and ignition requirements of an actual motor. The most serious difficulty is thet the ignitability data is obteined at constent heat flux and constant environmental pressure. In an actual motor firing, the igniter induced chamber pressure is normally transient, and heat flux may vary also, since it is a function of igniter mass flow rate.

Most logically, the ignition test deta should be compared with the everage igniter induced chamber pressure. Here, the average is taken from initiation up until some time, t, rather than using the average over the entire igniter function time. As far as the heet flux is concerned, it will be essentially constant for constant mass flow rate. And since flux is proportional to the four-fifths power of igniter mass flow rate, i.e., a power less than unity, the flux will be more neerly constant than the

mass flow rate itself. Hence, in many cases the approximation of constant heat flux is valid.

The interpretation given to the arc-image furnace ignition test data is as follows.

A sequence of ignitability tests are conducted. Over the sequence of tests the heat flux remains constant. But each test is conducted at a different level of environmental pressure. The result is a curve in the P_r vs t_π plane, where P_r is the pressure required for ignition, and t_π the time to ignition.

If the curve $\bar{P}_c$ vs t, where $\bar{P}_c$ is the time average igniter induced chamber pressure, is plotted in the same plane as P_r vs t_π, then the intersection of the two curves should be the time to ignition in an actual firing. The igniter induced heat flux must be, of course, equal to the flux at which the ignitability data was collected. These notions will be illustrated by a numerical calculation.

Time Average Igniter Induced Chamber Pressure: The average pressure up to time t is found from,

$$\bar{P}_c = \frac{1}{t} \int_0^t P_c(\tau)\, d\tau \qquad (23)$$

where

$\bar{P}_c$ = time average chamber pressure

P_c = chamber pressure

The igniter induced chamber pressure, P_c, is given in Eq. (22), and from this and Eq. (23),

$$\bar{P}_c = \frac{P_i}{at}(1 - e^{-at}) + \frac{1}{t}\int_0^t e^{-a\nu}\int_0^{\nu} e^{a\tau}\, b(\tau)\, d\tau\, d\nu \quad (24)$$

When the igniter mass flow rate is constant, Eq. (24) can be evaluated immediately, and is

$$\bar{P}_c = \frac{b}{a} + \frac{1}{at}\left(P_i - \frac{b}{a}\right)(1 - e^{-at}) \quad (25)$$

Minuteman Ignition: The motor has a grain configuration in the shape of a hollow cylinder with fins in the forward section, as shown in Figure (11). Ignition is by means of a controlled flow igniter, using propellant as the pyrotechnic. A total of six igniter port areas direct the flow into the finned region, and the areas of maximum heat flux will be located there. Hence, time to ignition must be calculated on the basis of flow into that region. Average gas temperature, however, will be calculated on the basis of flow into the cylindrical section, where the flux is assumed average. The hydraulic diameters in the two flow areas are,

$$d = \begin{cases} 10 \text{ inches, cylindrical section} \\ 1.5 \text{ inches, finned section} \end{cases}$$

Other motor parameters are,

$$V = 13{,}000 \text{ in.}^3$$

$$A_t = 73 \text{ in.}^2$$

$$A_b = 8000 \text{ in.}^2$$

$$A_f = 80 \text{ in.}^2$$

SCHEMATIC VIEW OF MOTOR PORT VOLUME

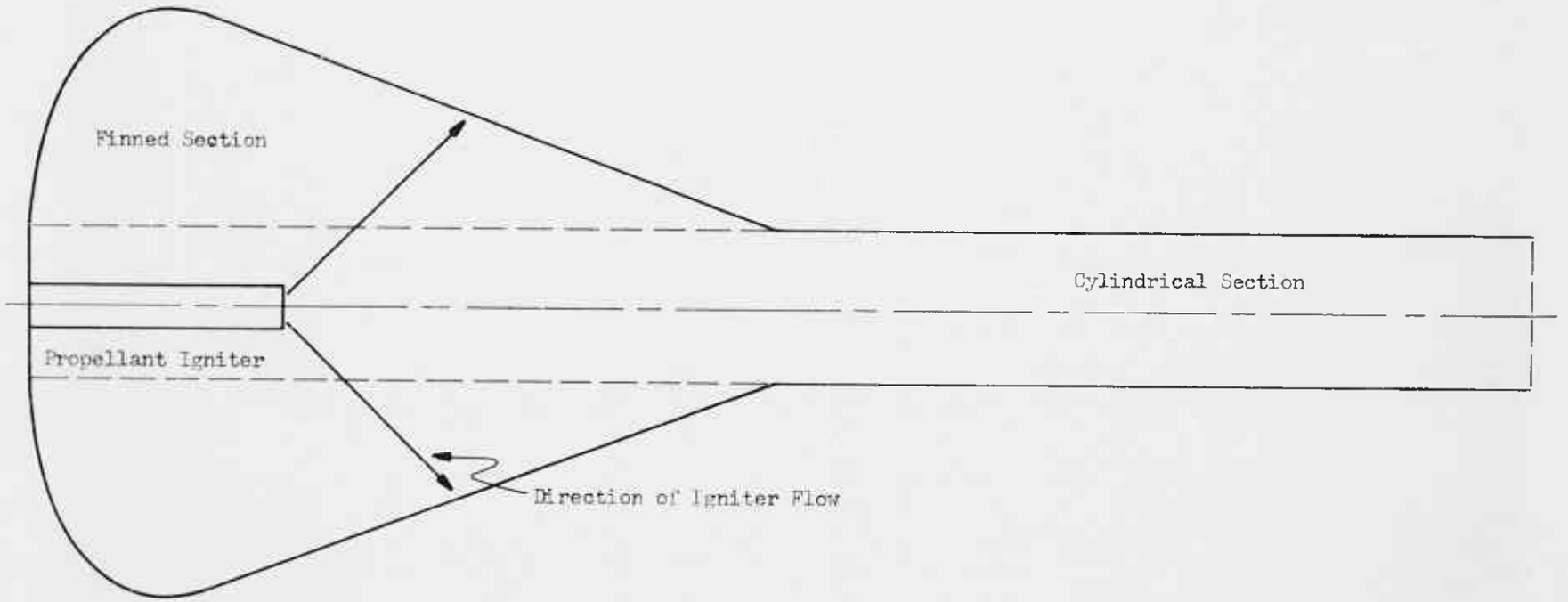

Figure (11)

Igniter and pyrotechnic constants are,

$\dot{m}_i$ = 8 lbs/sec, constant

$F = 3 \times 10^5$ ft-lbs/lb

$\gamma = 1.18$

t_o = 0.25 sec, total function time

m_i = 2 lbs, total charge weight

$\mu = 1.5 \times 10^{-6}$ lb-sec/ft^2, dynamic viscosity

The heat transfer parameter, Γ, (Eq. (16)), evaluating using the parameters listed above and in the cylindrical region, (d = 10 inches), has the value,

$$\Gamma = 0.415 \text{ (lbs/sec)}^{.2}$$

Average gas temperature ratio, θ_a, (Eq. (20), may be obtained then and is,

$$\theta_a = 0.67$$

Parameters occurring in the effective energy balance, Eq. (21), and their values are,

$$\dot{m}_e = \dot{m}_i - \Gamma \dot{m}_i^{.8} \theta_a = 6.53 \text{ lbs/sec}$$

$$a = \frac{F}{V} \gamma \sqrt{\theta_a} K A_t = 123 \text{ sec}^{-1}$$

$$b = \frac{F}{V} \dot{m}_e = 1810 \text{ lbs/in.}^2\text{sec}$$

For initial pressure near zero, the time average chamber pressure is from Eq. (25),

$$\bar{P}_c = \frac{b}{a} - \frac{b}{a^2 t}\left(1 - e^{-at}\right)$$

and using the values given above,

$$\bar{P}_c = 14.7 - \frac{120}{t}\left(1 - e^{-0.123t}\right), \text{ psia} \qquad (26)$$

$$0 \leq t \leq 250 \text{ msec.}$$

Heat flux for ignition, q, (Eq. (13)) is found from

$$\dot{q} = \frac{\Gamma' Q \dot{m}_i^{0.8} (\theta_a - \theta_s)}{A_s} \qquad (27)$$

where Γ' is the heat transfer parameter evaluated in the finned section, (d = 1.5 inches). For

$$Q = 1840 \text{ Btu/lb}$$

the value of the heat flux is,

$$\dot{q} = 257 \text{ Btu/ft}^2 \text{ sec} \sim 70 \text{ cal/cm}^2\text{sec}$$

On Figure (12), an ignition schematic is plotted for the case given above, with the propellant grain consisting of ANB-3066 LC. From the arc-image furnace ignition test data, curves have been obtained of pressure required for ignition vs time, for a flux of 70 cal/cm^{2}sec, for two types of surface preparation (Figure (6)). Recall in the computation given above, the heat flux for ignition was found equal to the ignitability test flux. By plotting the test data on the same graph as the curve $\bar{P}_c$ vs t the time

IGNITION SCHEMATIC - 70 CAL/CM^2 SEC - ANB-3066 LC

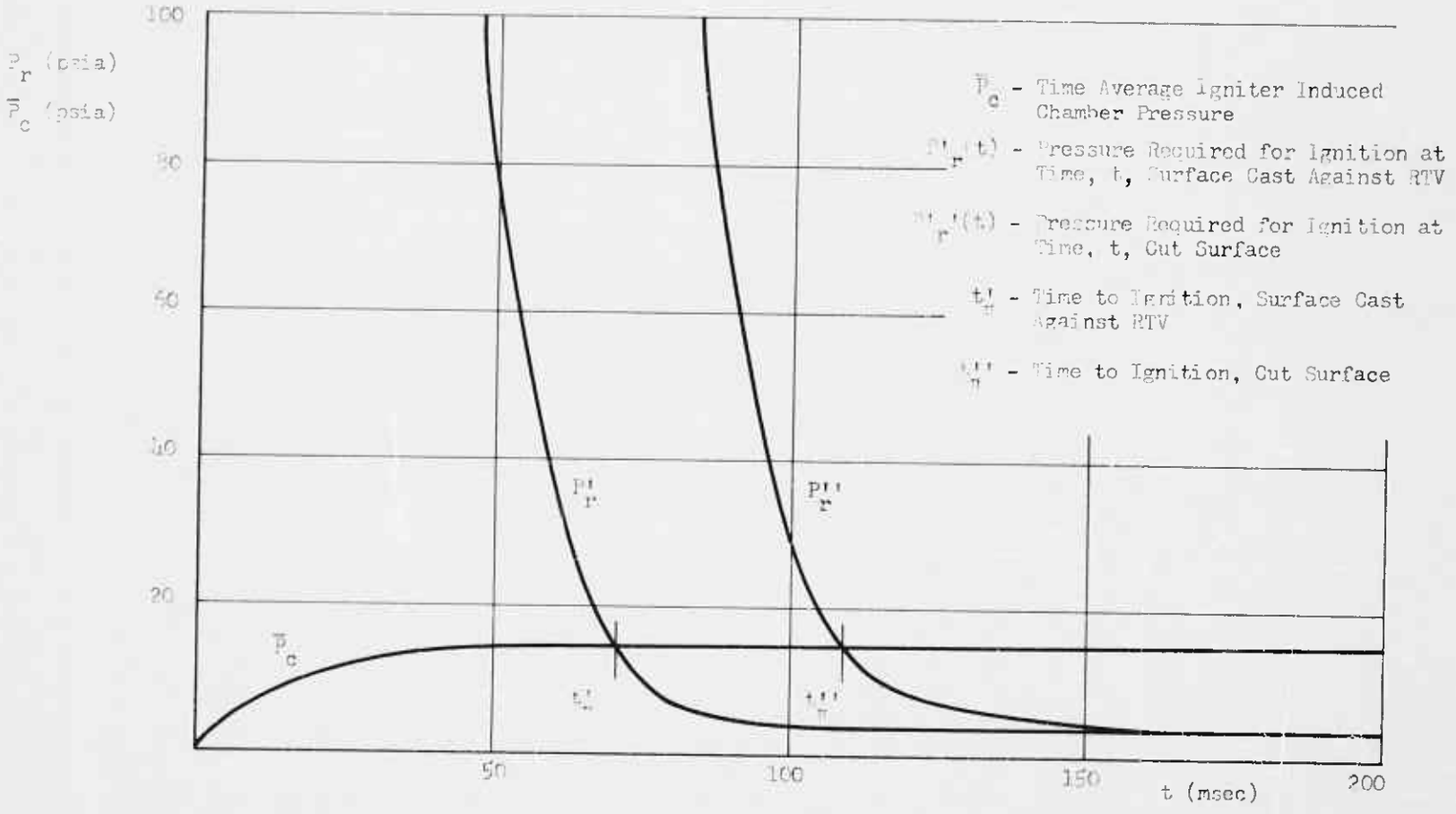

Figure (12)

to ignition is found as the intersection of the curves. This is evident from Figure (12).

Recapitulating, from motor, igniter, and pyrotechnic properties, the igniter induced motor pressure and heat flux were found. The igniter induced motor pressure was averaged over time, and compared with the pressure requirement for the condition of propellant ignition. The latter curve is experimentally obtained by ignitability measurements (Figure (6)), at a flux equal to that put out by the igniter. When the time averaged pressure curve equals the required pressure, ignition should occur.

A safety factor for motor ignition is defined as the ratio of igniter function time to ignition time. For the case of 2nd stage Minuteman, using ANB-3066 LC propellant cast against RTV, the safety factor based on a function time of 250 msec is,

$$S = \frac{250}{73} = 3.42$$

If the surface is scraped or cut, the safety factor is reduced to 2.3.

REFERENCES

1. B. L. Hicks and J. H. Frazer, "Thermal Theory of Ignition"; Bulletin of the 5th JANAF Meeting, March 1949.

2. E. W. Price, H. H. Bradley, Jr., and R. Fleming, "Ignition of Solid Propellants". Presented at Western States Section of the Combustion Institute, April 1963.

3. D. Altman and A. Grant, Jr., "The Thermal Theory of Ignition by Hot Wires"; Fourth Symposium on Combustion, 1953.

4. B. L. Hicks, "The Theory of Ignition Considered as a Thermal Reaction"; J. Chem. Phy. 22, No. 3, March 1954.

5. G. von Elbe and B. Lewis, "Theory of Ignition Threshold and a Program of Experimental Research on Propellant Ignition"; Bulletin of the 5th JANAF Meeting, March 1949.

6. Bermite Powder Company, Report No. 264, "Ignition Studies", January 8, 1962, prepared under Bureau of Naval Weapons, Contract 62-0236-C.

7. "Solid Propellant Ignition Studies with High Flux Radiant Energy as a Thermal Source", by R. B. Beyer and N. Fishman, Solid Propellant Rocket Research, Academic Press, 1960.

8. D. A. Frank - Kamenetskii, Diffusion and Heat Exchange in Chemical Kinetics, 1955.

9. H. W. Liepmann and A. E. Puckett, Aerodynamics of a Compressible Fluid, Wiley, 1947.

10. R. L. Lovine and B. E. Paul, "Status Report, Ignition Research", Aerojet-General Corporation, Sacramento, 1962.

11. W. H. Giedt, Principles of Engineering Heat Transfer, Van Nostrand, 1957.